Available online at www.sciencedirect.com
SCIENCE DIRECT®
International Journal of Heat and Mass Transfer 47 (2004) 4785–4794
International Journal of HEAT and MASS TRANSFER
www.elsevier.com/locate/ijhmt

Heat transfer from a circular cylinder to mixtures of water and ethylene glycol

S. Sanitjai, R.J. Goldstein *

Department of Mechanical Engineering, University of Minnesota, Heat Transfer Laboratory, 125, Mechanical Eng. Building, 111 Church Street SE, Minneapolis, MN 55455, USA

Received 30 July 2003; received in revised form 12 May 2004

Abstract

Local heat transfer by forced convection from a circular cylinder in crossflow is investigated for Reynolds number from 2×10^3 to 9×10^4 and Prandtl number from 7 to 176. The working fluids are water and mixtures of ethylene glycol and water. The cylinder is uniformly heated by passing a direct electric current through a thin surface heater. The influence of Reynolds number and Prandtl number on the distributions of local Nusselt number around a circular cylinder in crossflow is described.

Keywords: Local heat transfer; Circular cylinder; Reynolds number; Prandtl number; Water; Ethylene glycol

1. Introduction

While there have been many studies on local forced convection heat transfer from a circular cylinder to air, there have been few such studies using liquids. In this paper an experimental study of the local heat transfer coefficient distribution around a circular cylinder to liquids is described.

With air, Eckert and Soehngen [1], carried out experimental studies on the local heat transfer from a circular cylinder. Later Achenbach [2], Goldstein and Karni [3] (using mass transfer) extended the investigation over a large range of Reynolds number. In addition, the effects of surface roughness, free stream turbulence, thermal boundary condition and tunnel blockage on the local heat transfer from the cylinder were studied. Comprehensive reviews of many studies were published in [4,5].

Few studies have been conducted on local heat transfer from a cylinder to liquids. Generally liquid heat transfer studies have provided only overall heat transfer results.

Davis [6] measured the average heat transfer from wires to water, paraffin, and transformer oil for $0.14 < Re < 170$, $3 < Pr < 1.5\times10^3$ and $5 < \triangle T < 60$ °C. The wires were electrically heated, and heat loss to the fluids was measured. Perkins and Leppert [7] conducted an experiment in water and ethylene glycol covering $40 < Re < 10^5$, $1 < Pr < 300$ and $2.5 < \Delta T < 60$ °C. With a thermal boundary condition of uniform heat flux, overall heat transfer coefficients were obtained. Fand [8] measured the overall heat transfer coefficient from a cylinder to water for a uniform wall temperature boundary condition with $10^4 < Re < 10^5$, $Pr \approx 6$ and $2 < \Delta T < 6$ °C.

Perkins and Leppert [9] measured the local heat transfer from a cylinder to water for $2\times10^3 < Re < 1.2\times10^5$, $1 < Pr < 7$, $10 < \Delta T < 65$ °C and $0.208 < d/W < 0.415$. The effect of fluid property variations with temperature difference across the boundary layer were correlated using the factor $(\mu_w/\mu_b)^{0.25}$. Additionally,

* Corresponding author. Tel.: +1-612-625-5552; fax: +1-612-625-3434.
E-mail address: rjg@me.umn.edu (R.J. Goldstein).

0017-9310/$ - see front matter © 2004 Elsevier Ltd. All rights reserved.
doi:10.1016/j.ijheatmasstransfer.2004.05.013

Nomenclature

c_{p_f}	specific heat evaluated at T_f, J/kg K
d	diameter of the circular cylinder (25.4 mm in this study)
H	height of the liquid tunnel test section (180 mm in this study)
h	local convective heat transfer coefficient, W/m^2 K
$\overline{h}$	average heat transfer coefficient, W/m^2 K
I	electric current, A
k_f	thermal conductivity evaluated at T_f, W/m K
L	length of heated section of test cylinder (165 mm in this study)
L_h	axial distance for voltage drop measurement (100 mm in this study)
Nu	Nusselt number, $Nu = \frac{hd}{k_f}$
$\overline{Nu}$	average Nusselt number, $\overline{Nu} = \frac{\overline{h}d}{k_f}$
Pr	Prandtl number, $Pr = \frac{\mu_f c_{p_f}}{k_f}$
$\dot{q}_{cd}$	conduction heat flux based on surface area of heater, W/m^2
$\dot{q}_{cv}$	convective heat flux based on surface area of heater, W/m^2
$\dot{q}_{gen}$	energy dissipation per unit surface area of heater, W/m^2
Re	Reynolds number based on a diameter and incoming velocity, $Re = \frac{\rho_f U d}{\mu_f}$
T_b	bulk temperature, K
T_d	dynamic temperature, $T_d = \frac{U^2}{2c_{p_f}}$, K
T_f	film temperature, $T_f = 0.5(T_\infty + T_w)$, K
T_t	total temperature, K
T_w	wall temperature, K
T_∞	free stream temperature, K
ΔT	temperature difference ($T_w - T_\infty$)
U	approaching velocity, m/s
V	voltage drop across heater, V
$\hat{V}_{EG}$	volume of ethylene glycol in liquid tunnel, m^3
$\hat{V}_T$	volume of mixture in liquid tunnel ($\approx$2 m^3 in this study)
W	width of the test section (180 mm in this study)

Greek symbols

θ	angle around the cylinder, $\theta = 0°$ at front stagnation line
μ_b	dynamic viscosity evaluated at T_b, kg/m s
μ_f	dynamic viscosity evaluated at T_f, kg/m s
μ_w	dynamic viscosity evaluated at T_w, kg/m s
ρ_f	density evaluated at T_f, kg/m^3

they found that the blockage of the tunnel has a significant effect on the local heat transfer because of its influence on the velocity distribution. Zukauskas [10] published the results of local heat transfer from a circular cylinder to air, water, and transformer oil. The effects of fluid property variations in the boundary layer on heat transfer were included using factor $(Pr_b/Pr_w)^{0.25}$. Most of his results presented were for the average heat transfer.

Vilimpoc et al. [11] did experiments within $0.0002 < Re < 64$ and $5.5 < Pr < 2.7 \times 10^4$. With a small ΔT of 0.1 °C, the variations in fluid properties in the boundary layer are negligible. Local heat transfer around a cylinder was investigated using a holographic technique. With a low Pr fluid, an experiment and numerical predictions were performed by Ishiguro et al. [12] using liquid-sodium with $220 < Re < 1.7 \times 10^4$, $5.8 \times 10^{-3} < Pr < 7.3 \times 10^{-3}$.

The local heat transfer around a circular cylinder to liquid is not clearly understood due to limited available results and significant differences in the experimental conditions of the previous studies. The objective of this study is to systematically determine the local heat transfer coefficient around a circular cylinder in liquid and provide base-line data that would aid in predicting heat transfer around a circular cylinder to various fluids. The Prandtl number dependence on local heat transfer around a circular cylinder is investigated.

2. Experimental apparatus

2.1. Flow system

A schematic diagram of the recirculating liquid-flow tunnel used in this experiment is shown in Fig. 1. It is a closed loop tunnel with a total fluid capacity of about 2 m^3. The recirculating duct has a 400 mm diameter including four turning elbows containing guide vanes. The liquid pumped by an impeller flows through anti-rotation blading and a diffuser to the recirculating duct. Then the liquid flows through a bubble trap section and a row of screens and enters a contraction section with an area ratio of 4:1. The test section is a square duct with 180×180 mm cross-section and 1060 mm length. It is made of 25 mm thick Plexiglas. The bottom wall of the test section has a support plate which is used to hold the test cylinder. The downstream end of the test section is connected to a diffuser which has an area ratio of 1:2. The velocity in the test section is measured using a 3-hole impact probe connected to two Merriam Red-oil manometers. The test section velocity can be varied from 1.5 to about 5 m/s by changing the shaft-speed of the pump. The velocity distribution across the test section is measured and found to be uniform. Free stream turbulence intensity is less than 0.5%. The temperature of the liquid in the tunnel is recorded during the experiment

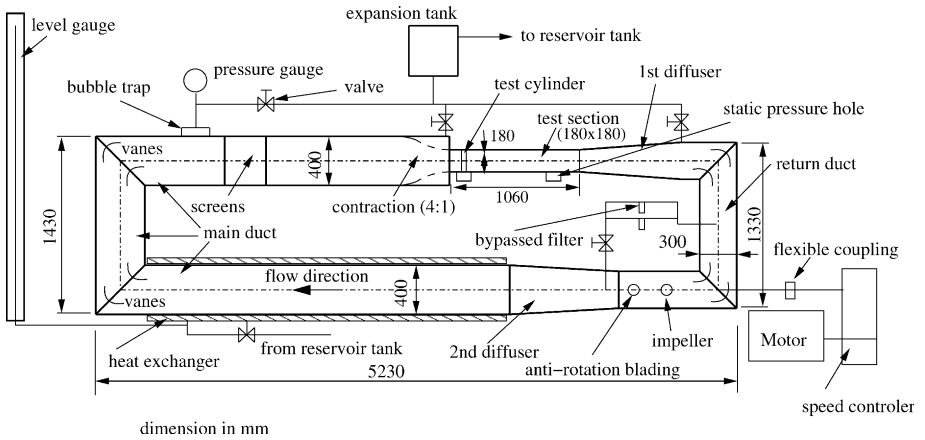

Fig. 1. Liquid tunnel.

and maintained constant (±0.5 °C) by manually adjusting the water flow rate through a heat exchanger.

2.2. Test cylinder

The test cylinder with 25.4 mm diameter and 200 mm length, Fig. 2, is vertically placed 15 cm from the exit of the contraction. The blockage ratio (d/W) of the cylinder in the test section is 0.14. The test cylinder is made mainly of Styrofoam ($k \approx 0.026$ W/m K) to minimize heat flow by conduction. The external surface of the test cylinder consists of an Inconel 600 foil wrapped around an electrically insulated phenolic tube of 1 mm wall thickness which tightly slides over the Styrofoam. The foil of 25.4 μm thickness is attached on the phenolic tube using 25.4 μm thick double-side adhesive and is heated by supplying an electric current through copper connectors at both ends of the cylinder. Silver-paint connects the Inconel foil heater with the copper connectors.

Surface temperatures are measured with eight T-type (copper-constantan) thermocouples installed under the heating surface in grooves cut in the phenolic tube. The junctions of these thermocouples are flush with the phenolic tube surface as shown in Fig. 2. To measure the local surface temperatures at a given θ, the test cylinder is rotated in five degrees intervals using a protractor. The free stream total temperature (T_t) is obtained from a thermocouple installed in the contraction section and its measured profile is uniform across the section.

A direct current power supply, HP model 6032A with maximum power of 1000 W, is used. Voltage drops (V) across the heating element on the phenolic tube are measured using tap wires, Fig. 2, attached to the Inconel foil by small drops of silver-paint. The current is

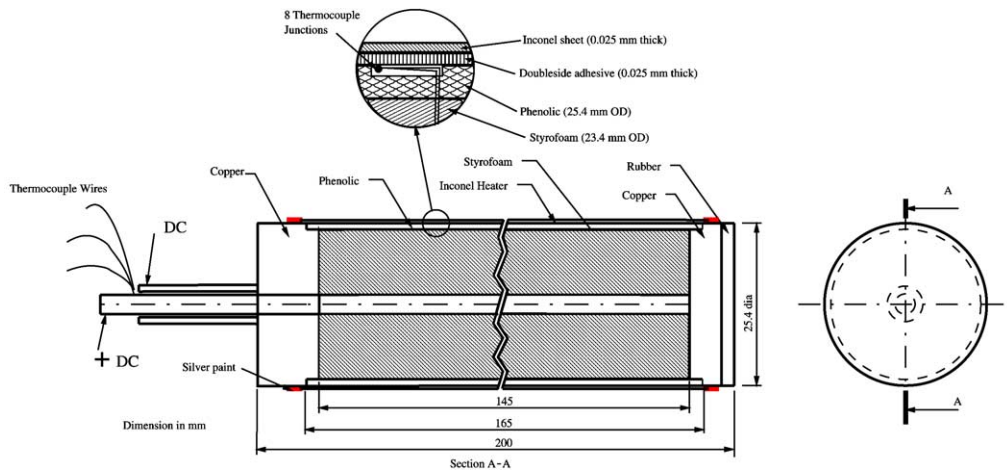

Fig. 2. Test cylinder.

determined by measuring the voltage drop across standard resistors. Using a computer control program, the electric current (I) was maintained constant.

3. Experimental technique

A constant heat flux boundary condition is employed in this study. The local convective heat transfer coefficient is calculated as:

$$h = \frac{\dot{q}_{cv}}{T_w - T_{aw}} \tag{1}$$

$\dot{q}_{cv}$ is the net convective heat flux from the outer surface of the cylinder, T_w is the local surface temperature, and T_{aw} is the local adiabatic temperature. Since the dynamic temperature of liquid flow is small ($0.0005\ ^\circ\text{C} < T_d < 0.006\ ^\circ\text{C}$), the adiabatic wall temperature is closely equal to the free stream total temperature (T_t).

The net convective heat transfer rate per unit surface area ($\dot{q}_{cv}$) from the test cylinder surface is determined as:

$$\dot{q}_{cv} = \dot{q}_{gen} - \dot{q}_{cd} \tag{2}$$

where $\dot{q}_{gen}$ is a uniform heat generation rate per unit surface area in the Inconel foil and $\dot{q}_{cd}$ is a conduction heat loss per unit surface area which is corrected for each circumferential location on the cylinder surface. The heat loss by conduction from the Inconel foil heater to the inner core and the ends of the test cylinder is determined using the numerical program CONDUCT by Patankar [13]. In this experiment only the heat transfer in the two-dimensional flow regime (i.e. away from the top and bottom walls of the test section) is considered. The maximum correction for conduction heat loss is about 3% of $\dot{q}_{gen}$ near $\theta = 85^\circ$.

The heat generation rate per unit surface area is determined from:

$$\dot{q}_{gen} = \frac{V \cdot I}{\pi d \cdot L_h} \tag{3}$$

where I is the electric current calculated from the voltage drop across standard resistors for high current of 40–50 A, and V is the voltage drop across the axial distance L_h.

The experimental uncertainty evaluated based on the 95% confidence level was analyzed using the method described in [14]. The uncertainty of the heat transfer coefficient is 3.6%.

3.1. Working fluids

The experiments were conducted using water and six mixtures of ethylene glycol and water. The mixture concentrations ($\hat{V}_{EG}/\hat{V}_T$) are 25.1%, 40.7%, 64.5%, 81.5%, 89.7% and 97.8%. The range of the Prandtl number is from 7 to 176, and the range of the Reynolds number is from 2×10^3 to 9×10^4. Due to a significant change on thermophysical properties of the liquids with temperature, all thermophysical properties are evaluated at the film temperature (T_f) to account for the temperature variations in the boundary layer. The densities of mixtures of ethylene glycol and water at various concentrations are measured using precision hydrometers. The viscosities of the liquids are measured using a Brookfield viscometer model DV-E equipped with an Ultra-Low adapter. The specific heat (c_{p_f}) and the thermal conductivity (k_f) of the mixtures are obtained from [15].

The experimental conditions for the test runs are summarized in Table 1.

4. Experimental results

Flow visualization in water was conducted using an alcohol-milk mixture injected through the cylinder into the flow at $\theta = 5 \pm 0.2^\circ$. Fig. 3 shows the flow pattern around the cylinder at $Re \approx 4.5 \times 10^4$ ($U_\infty = 1.75$ m/s). On the front part of the cylinder, the flow smoothly moves downstream indicating a laminar boundary layer. The dye line becomes thicker showing growth of the boundary layer with θ. The boundary layer separates from the surface of the cylinder at about 90°. Down-

Table 1
Working fluids and ranges of the Reynolds number and the Prandtl number

Ethylene glycol concentration	Reynolds number	Prandtl number	U_∞ (m/s)	T_∞ (°C)	ΔT (°C)
Water	45,000–90,000	6.5–7.5	1.7–3.6	21–23	1.2–2.5
25.1%	21,000–53,800	14–16	1.7–4.0	16.9–20.4	1.2–3.0
40.7%	15,200–38,100	21–24	1.7–3.9	19.5–23.2	1.1–2.7
64.5%	8,800–23,300	44–49	1.6–4.3	17.3–23.7	1.1–2.5
81.5%	4,000–10,500	87–91	1.5–4.1	14.5–19.8	1.1–4.3
89.7%	2,600–10,300	100–146	1.5–3.8	18.2–19.6	1.1–6.1
97.8%	2,200–8,400	146–176	1.5–4.0	18.5–21.3	1.1–7.2

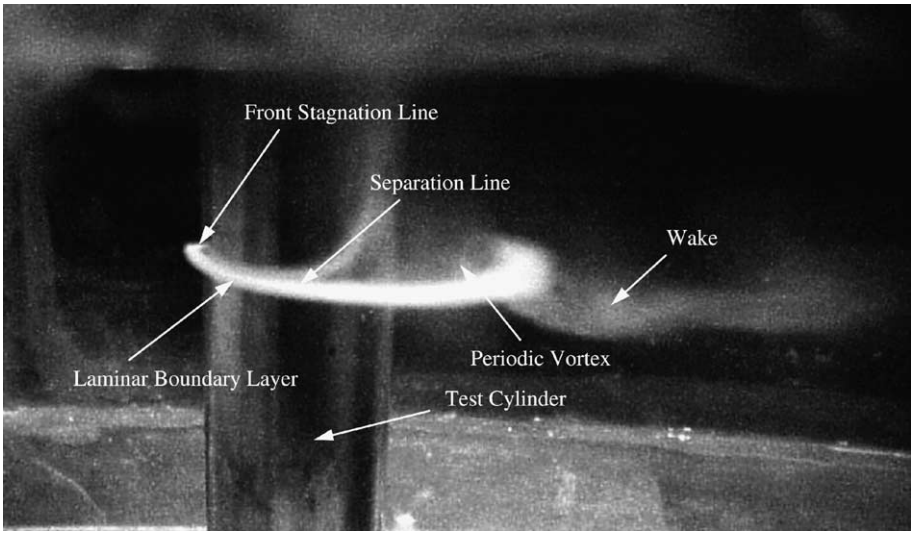

Fig. 3. Flow visualization in water.

stream of separation, the dye line has a curved shape formed by a reverse periodic vortex.

Heat transfer results are presented in the form of the dimensionless Nusselt number which is calculated as:

$$Nu = \frac{h \cdot d}{k_f} \tag{4}$$

Effects of the Reynolds number and the Prandtl number on local heat transfer are described below.

4.1. Effects of the Reynolds number

The effects of the Reynolds number can be observed in Figs. 4–8. Generally, the tests in each plot have nearly the same Prandtl number. The experiments with low Prandtl number mixtures have high Reynolds numbers due to the lower viscosity of the working fluids. The ranges of Reynolds number for seven working fluids overlap each other. This study covers Reynolds numbers from 2×10^3 to 9×10^4.

As expected, the heat transfer rate increases as the Reynolds number increases. The distribution of the local Nusselt number depends on the Reynolds number range. Figs. 4–8 show the distributions of the local Nusselt number in water, and in 25.4%, 64.5%, 89.7%and 97.8% mixtures of ethylene glycol and water. With $Re > 5 \times 10^3$, the distributions of the local Nusselt number have similar trends for all Reynolds numbers. At this Reynolds number, the distribution can be divided into three regions. In the first region ($0° < \theta \leqslant 85°$) the Nusselt number monotonically declines from the front stagnation point and reaches a minimum at 85° due to the growth of the thermal boundary layer which increases the thermal resistance. The increase of the

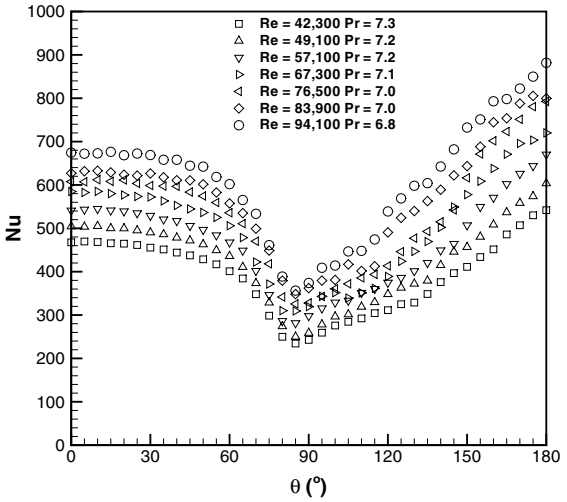

Fig. 4. Distribution of local Nusselt number at $Pr \approx 7$.

Nusselt number with θ in the second region ($85° < \theta \leqslant 135°$) is caused by the reattachment of the free shear layer. The cylinder surface in this region is covered by the reattached flow which brings fresh fluid close to the surface of the cylinder. In the third region ($135° < \theta \leqslant 180°$), the approximately linearly increase in heat transfer in the downstream direction is caused by reverse periodic vortices.

With $Re < 5 \times 10^3$, the heat transfer is approximately constant in the region of $90° < \theta < 180°$. There is no hump, as with $Re > 5 \times 10^3$, in the region of $90° < \theta < 135°$. It is expected that the cylinder surface in this region is covered by the reverse flow produced by the

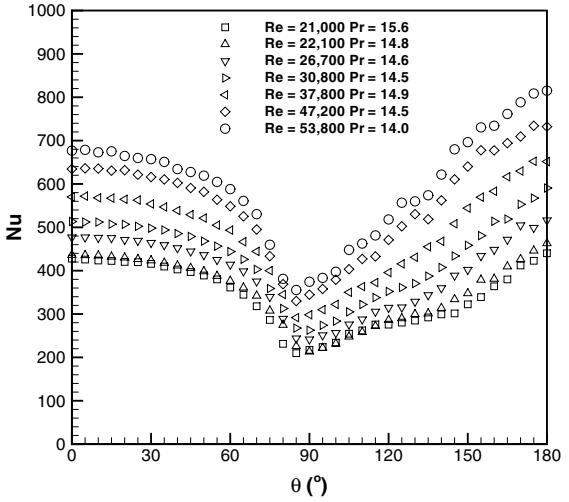

Fig. 5. Distribution of local Nusselt number at $Pr \approx 15$.

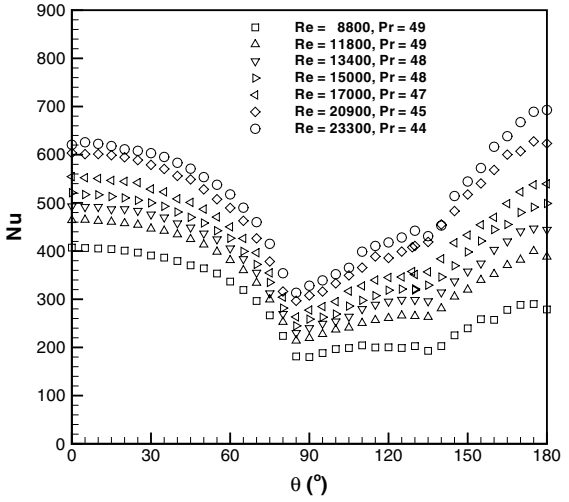

Fig. 6. Distribution of local Nusselt number at $Pr \approx 45$.

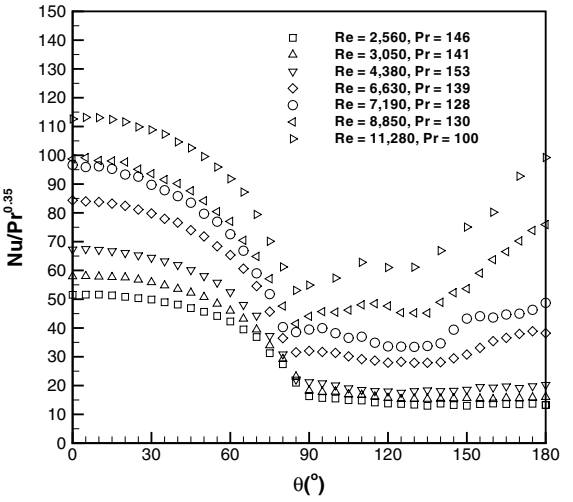

Fig. 7. Distribution of local Nusselt number at $Pr \approx 140$.

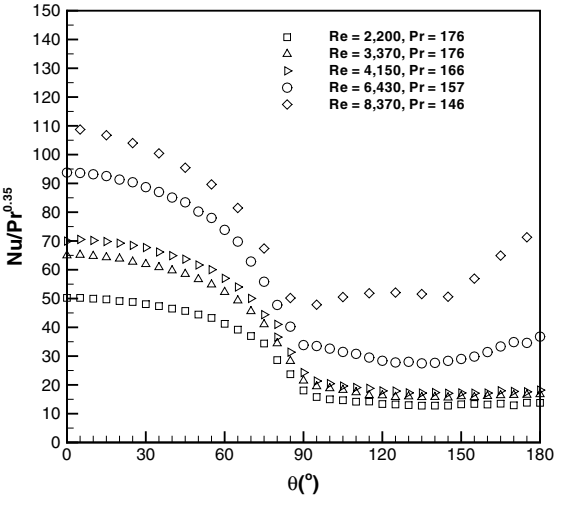

Fig. 8. Distribution of local Nusselt number at $Pr \approx 170$.

periodic vortices [16]. Schlichting [17] reported that only in the range of $60 < Re < 5 \times 10^3$ is a regular Karman steet observed. Zdravkovich [18] described that length of the eddy formation region is long for low Reynolds number. The strength of the periodic vortices is too subtle to bring fresh fluid close to the heated surface, so the heat transfer is almost constant. When the Reynolds number is larger than 5×10^3, the development of the second and the third regions for $\theta > 85°$ can be observed. The length of eddy formation region significantly decreases with the Reynolds number for $Re > 5 \times 10^3$, [18]. Length of transition from laminar to turbulent free shear layer also decreases with Reynolds number and reaches the separation point at $Re \approx 4 \times 10^4$. After the separation point a hump, in the region of $90° < \theta < 135°$ for $Re > 4 \times 10^4$, vanishes because all regions in the free shear layer are turbulent.

The distributions of the normalized Nusselt number $[Nu/(Re^{0.5})]$ around the cylinder for 40.7% and 81.5% mixtures are shown in Figs. 9 and 10. In the front part ($0° < \theta < 85°$) in Fig. 9 the distributions are similar and the data collapse onto a single curve in the region from $\theta = 0°$ to $\theta = 60°$. Thus, the local Nusselt number in that region is closely proportional to $Re^{0.5}$ as one might expect for a laminar boundary layer. Downstream of $\theta = 60°$ in Fig. 9 data deviate somewhat from a single curve. For $Re = 9100$ and 10,470 in Fig. 10, $Nu/(Re^{0.5})$ is higher than that at lower Reynolds number due to the

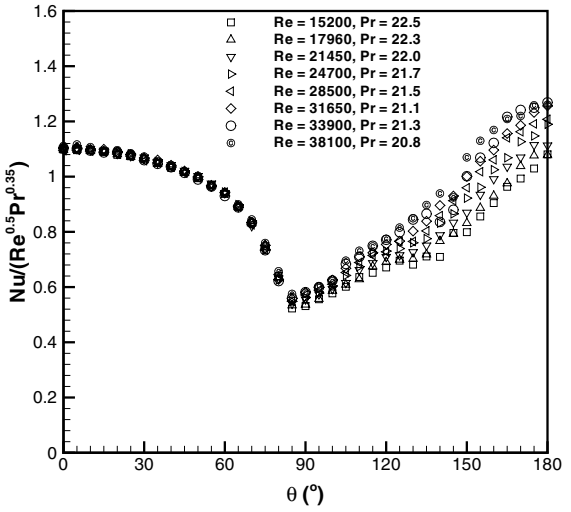

Fig. 9. Distribution of local normalized Nusselt number at $Pr \approx 22$.

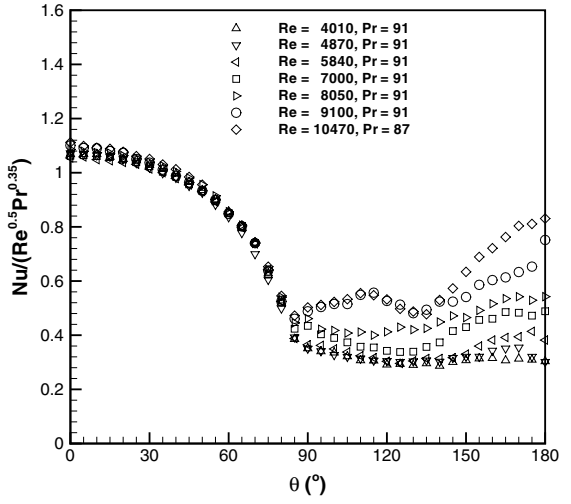

Fig. 10. Distribution of local normalized Nusselt number at $Pr \approx 91$.

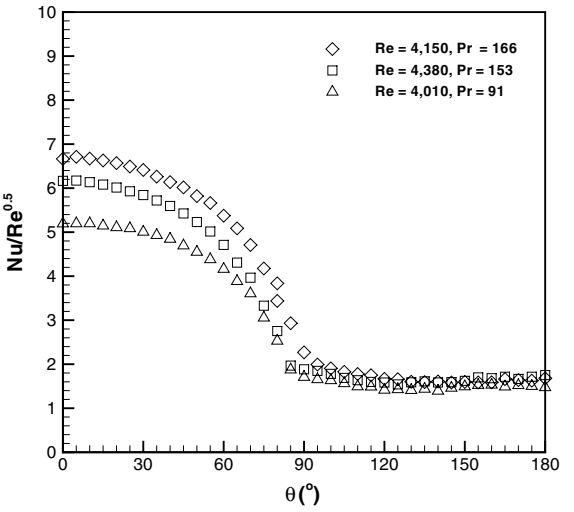

Fig. 11. Distribution of local Nusselt number at $Re \approx 4 \times 10^3$.

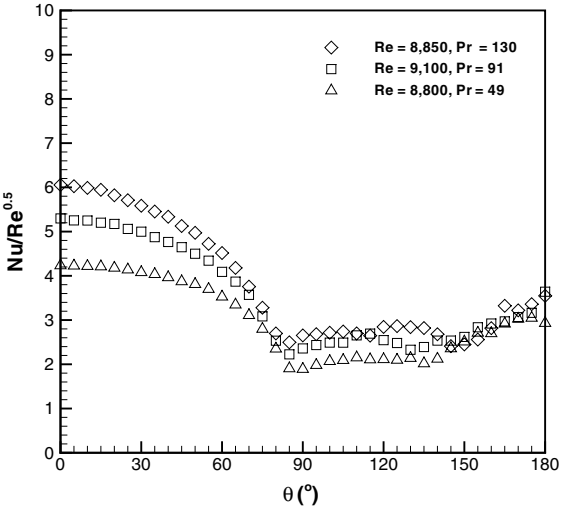

Fig. 12. Distribution of local Nusselt number at $Re \approx 9 \times 10^3$.

effect of alternating vortex flow behind the cylinder and a decrease in length of the eddy formation region.

4.2. Effects of the Prandtl number

The distributions of the local Nusselt number with different Prandtl number at roughly the same Reynolds number are shown in Figs. 11–13. Generally, the local Nusselt number increases as the Prandtl number increases. As can be seen in Fig. 11, on the front part of the cylinder ($0° < \theta < 90°$) the local Nusselt number is strongly affected by the Prandtl number. The Nusselt number at the front stagnation point ($\theta = 0°$) increases about 30% as the Prandtl number increases from 91 to 166 at $Re \approx 4 \times 10^3$. However, on the rear part of the cylinder ($90° < \theta < 180°$) the effect of the Prandtl number on the local Nusselt number is comparatively small. The local Nusselt number in that region is constant in a narrow range from about 100 to 110 for the Prandtl numbers plotted.

At $Re \approx 9 \times 10^3$, Fig. 12 shows that in the front part of the cylinder the local Nusselt number is again strongly affected by the Prandtl number. In the reattachment region of $90° < \theta < 150°$, the effect of the Prandtl number can be observed and the local Nusselt

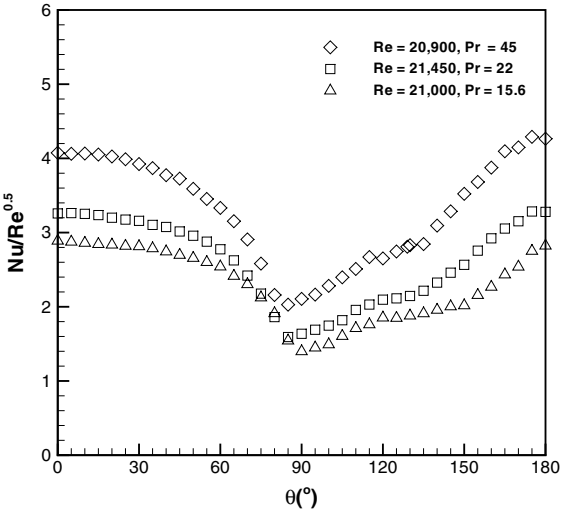

Fig. 13. Distribution of local Nusselt number at $Re \approx 21 \times 10^4$.

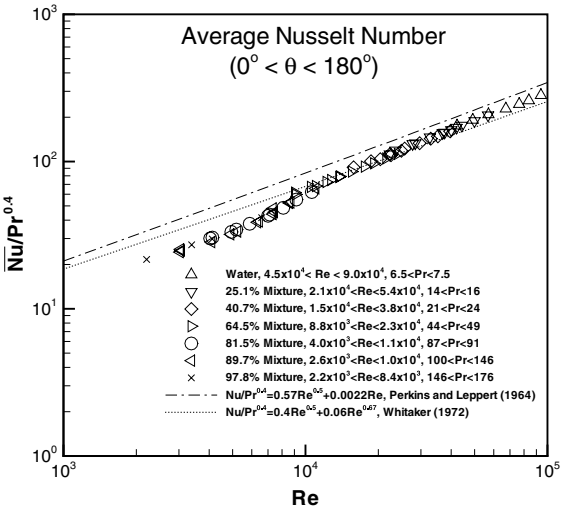

Fig. 14. Average Nusselt number around a circular cylinder.

number in this region increases as the Prandtl number increases. However, in the region of $150° < \theta < 180°$ the effect of the Prandtl number is small and the local Nusselt number in this region is approximately same for $Pr = 49, 91$, and 130.

The effects of the Prandtl number at $Re \approx 2.1 \times 10^4$ are shown in Fig. 13. The effects of the Prandtl number on the local Nusselt number on the front and rear parts of the cylinder are similar when the Reynolds numbers are higher than 10^4; the Nusselt number at every location increases with increasing Prandtl number.

From the results shown in Figs. 11–13, it can be concluded that the effects of the Prandtl number depend on the flow characteristics around the circular cylinder. With $Re < 5 \times 10^3$, the Prandtl number mainly affects the local Nusselt number in the region where the laminar boundary layer exists. The effect of the Prandtl number in the region downstream of the separation point is comparatively small. With $5 \times 10^3 < Re < 10^4$, the local Nusselt number in both the laminar boundary layer region and the reattachment flow region is significantly affected by the Prandtl number, but only a small effect can be observed in the periodic wake region. When the Reynolds number is greater than 10^4, the local Nusselt number in every region on the cylinder is affected by the Prandtl number.

4.3. Average heat transfer

The average Nusselt number around the circular cylinder ($0° < \theta < 180°$) is shown in Fig. 14. The correlations by Perkins and Leppert [9] and Whitaker [19] are also shown in the figure. The present experimental results agree well with the correlation by Whitaker [19] for $Re > 10^4$. However, for $Re < 10^4$ the experimental results are lower than other predictions because the contribution of heat transfer on the rear part of the cylinder is lower than the front part of the cylinder for this range of Reynolds number. The effect of the tunnel blockage on the average Nusselt number for $d/W = 0.14$ is about 3% as reported in [9]. A correlation for predicting the overall Nusselt number is presented in [20].

5. Comparison with other results

The Nusselt number results are compared with those from other studies in Fig. 15. Generally, on the front

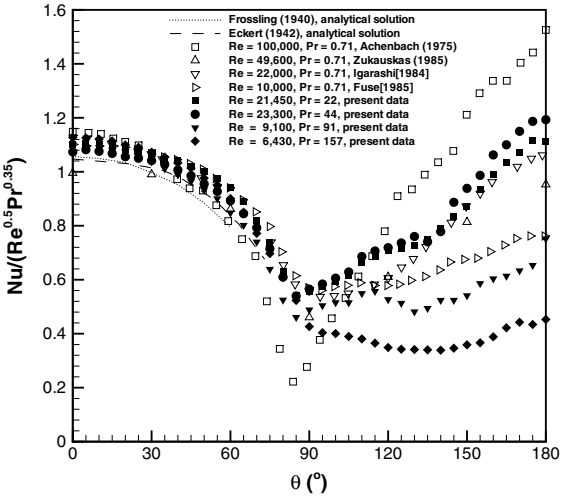

Fig. 15. Comparison with other results.

part ($0° < \theta < 60°$) of the cylinder the present data agree well with the analytical results of [21,22] and with experimental heat transfer results of [2,5,23,24]. The present results at $Re = 9100$ and 21,450 for $0° \leqslant \theta \leqslant 180°$ have a fair agreement with the results of [23,24], respectively. Downstream of $\theta = 60°$ the results of [2] under the uniform temperature boundary condition decline faster than the present results. This may be due to the different thermal boundary conditions. The effect of the thermal boundary condition was also reported in [25].

The results on the rear part ($90° < \theta < 180°$) of the cylinder deviate due to various effects such as the Reynolds number, the Prandtl number, the thermal boundary condition and the blockage ratio.

6. Summary and conclusions

The present study provides information on local heat transfer from a circular cylinder in crossflow to liquids over the range of $2 \times 10^3 < Re < 9 \times 10^4$ and $7 < Pr < 176$. Local heat transfer results were obtained under the boundary condition of uniform heat flux. Heat transfer around a cylinder is strongly affected by the Reynolds number and the Prandtl number. The distribution of local heat transfer changes with the range of Reynolds number. On the front part ($0° < \theta < 85°$) of the cylinder, local heat transfer increases with increasing Prandtl number. However, on the rear part ($85° < \theta < 180°$), local heat transfer depends on flow characteristics near the surface. With $Re < 5 \times 10^3$ the effect of the Prandtl number on heat transfer downstream of the separation point is small. The Nusselt number is approximately constant after the separation point. With $Re > 5 \times 10^3$, the local heat transfer increases with the Prandtl number.

Acknowledgements

Support from the Engineering Research Program of the Office of Basic Energy Science at the US Department of Energy and from the King Mongkut's University of Technology Thonburi (KMUTT) in the form of a fellowship for S. Sanitjai is gratefully acknowledged.

References

[1] E. Eckert, E. Soehngen, Distribution of heat-transfer coefficients around circular cylinders in crossflow at Reynolds numbers from 20 to 500, Trans. ASME 74 (1952) 343–347.

[2] E. Achenbach, Total and local heat transfer from a smooth circular cylinder in crossflow at high Reynolds number, Int. J. Heat Mass Transfer 18 (1975) 1387–1396.

[3] R.J. Goldstein, J. Karni, The effect of a wall boundary layer on local mass transfer from a cylinder in crossflow, J. Heat Transfer 106 (1984) 260–267.

[4] V.T. Morgan, The overall convective heat transfer from smooth circular cylinders, Adv. Heat Transfer 11 (1975) 199–264.

[5] A.A. Zukauskas, J. Ziugzda, Heat Transfer of a Cylinder in Crossflow, Hemishere Pub, Washington, New York, 1985.

[6] A.H. Davis, Convective cooling of wires in streams of viscous liquid, Phil. Mag. 47 (1924) 1057–1092.

[7] H.C. Perkins, G. Leppert, Forced convection heat transfer from a uniformly heated cylinder, J. Heat Transfer 84 (1962) 257–263.

[8] R.M. Fand, Heat transfer by forced convection from a cylinder to water in crossflow, Int. J. Heat Mass Transfer 8 (1965) 995–1010.

[9] H.C. Perkins, G. Leppert, Local heat-transfer coefficients on a uniformly heated cylinder, Int. J. Heat Mass Transfer 7 (1964) 143–158.

[10] A.A. Zukauskas, Heat transfer from tubes in cross-flow, Adv. Heat Transfer 8 (1972) 93–160.

[11] V. Vilimpoc, R. Cole, P.C. Sukanek, Heat transfer in Newtonian liquids around a circular cylinder, Int. J. Heat Mass Transfer 33 (1990) 447–456.

[12] S. Ishiguro, K. Sugiyama, T. Kumada, Heat transfer around a circular cylinder in liquid-sodium crossflow, Int. J. Heat Mass Transfer 22 (1979) 1041–1048.

[13] S.V. Patankar, Computation of Conduction and Duct Flow Heat Transfer, Innovative Research, Maple Grove, MN, 1991.

[14] H.W. Coleman, W.G.J. Steele, Experimentation and Uncertainty Analysis for Engineers, Wiley, New York, 1989, pp. 75–118.

[15] R.W. Gallant, C.L. Yaws, Physical Properties of Hydrocarbons, Gulf Pub, Houston, 1993.

[16] M. Lebouche, M. Martin, Convection forcee autour du cylindre; sensibilite aux pulsations de l'ecoulement externe, Int. J. Heat Mass Transfer 18 (1975) 1161–1175.

[17] H. Schlichting, Boundary-Layer Theory, seventh ed., McGraw-Hill Book Company, New York, 1979.

[18] M.M. Zdravkovich, Flow Around Circular Cylinders, Oxford University Press Inc., New York, 1997, pp. 94–162.

[19] S. Whitaker, Forced convection heat transfer calculations for flow in pipes, past flat plate, single cylinder, and for flow in packed beds and tube bundles, AIChE J. 18 (1972) 361–371.

[20] S. Sanitjai, R.J. Goldstein, Forced convection heat transfer from a circular cylinder in crossflow to air and liquids, Int. J. Heat Mass Transfer 47 (2004).

[21] N. Frossling, Evaporation, heat transfer, and velocity distribution in two dimensional and rotationally symmetrical laminar boundary-layer flow, Acta Univ. Lund: English Translation, NACA TM 1432, 1958 2.

[22] E.R.G. Eckert, Die bereshnung des warmeuberganges in der laminaren grenzschicht umstromter korper, VDI-Froschungshefl 416 (1942) 1–26.

[23] T. Igarashi, Correlation between heat transfer and fluctuating pressure in separated region of a circular cylinder, Int. J. Heat Mass Transfer 27 (6) (1984) 927–937.
[24] H. Fuse, T. Oyama, S. Kanamori, Influence of free-stream turbulence on heat transfer at the rear surface of a cylinder (effects of high frequency turbulence), Heat Transfer—Japanese Research 14 (3) (1985) 1–20.
[25] J.W. Baughn, N. Saniei, The effect of the thermal boundary condition on heat transfer from a cylinder in crossflow, J. Heat Transfer 113 (1991) 1020–1023.